

EGU, Sharing Geosciences online 2020

A small-scale numerical study of fault slip mechanisms using DEM

Nathalie Casas^{1,2}, Guilhem Mollon^{1,3}, and Ali Daouadji²

**nathalie.casas@insa-lyon.fr*

¹LaMCoS, INSA Lyon/University of Lyon/CNRS UMR5259, Bâtiment Sophie Germain, 27bis Avenue Jean Capelle, 69621 Villeurbanne Cedex, France

²GEOMAS, INSA de Lyon/University of Lyon, Bâtiment J.C.A. Coulomb, 34 avenue des Arts, 69621 Villeurbanne Cedex, France

³Laboratoire de Géologie, École Normale Supérieure/CNRS UMR 8538, PSL Research University, 24 rue Lhomond, F-75005 Paris, France

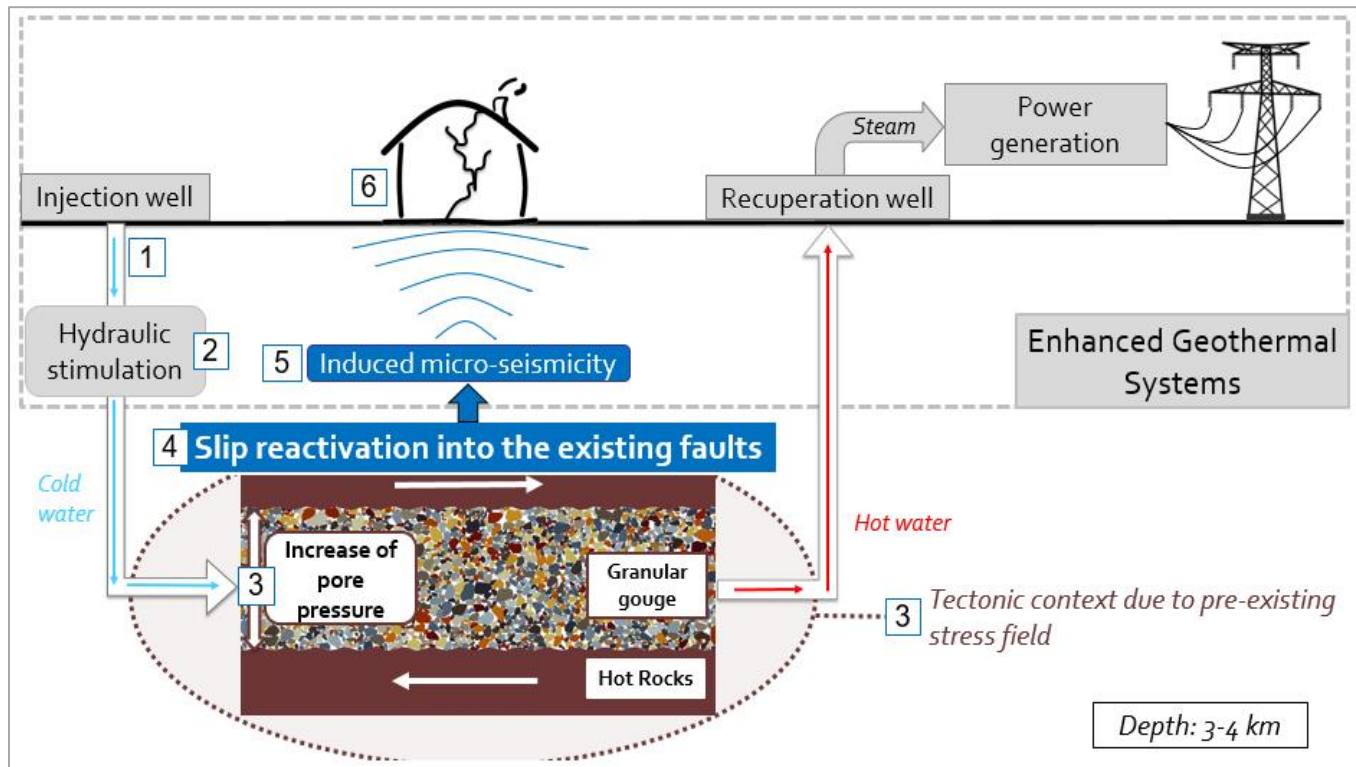
Presentation made with previous and new results. Lots of text, to facilitate comprehension without live presentation.

1. Introduction - Context
2. Sample generation and numerical modelling
3. Results on granular gouge behaviour
4. Perspectives and conclusions

1- Introduction - Context

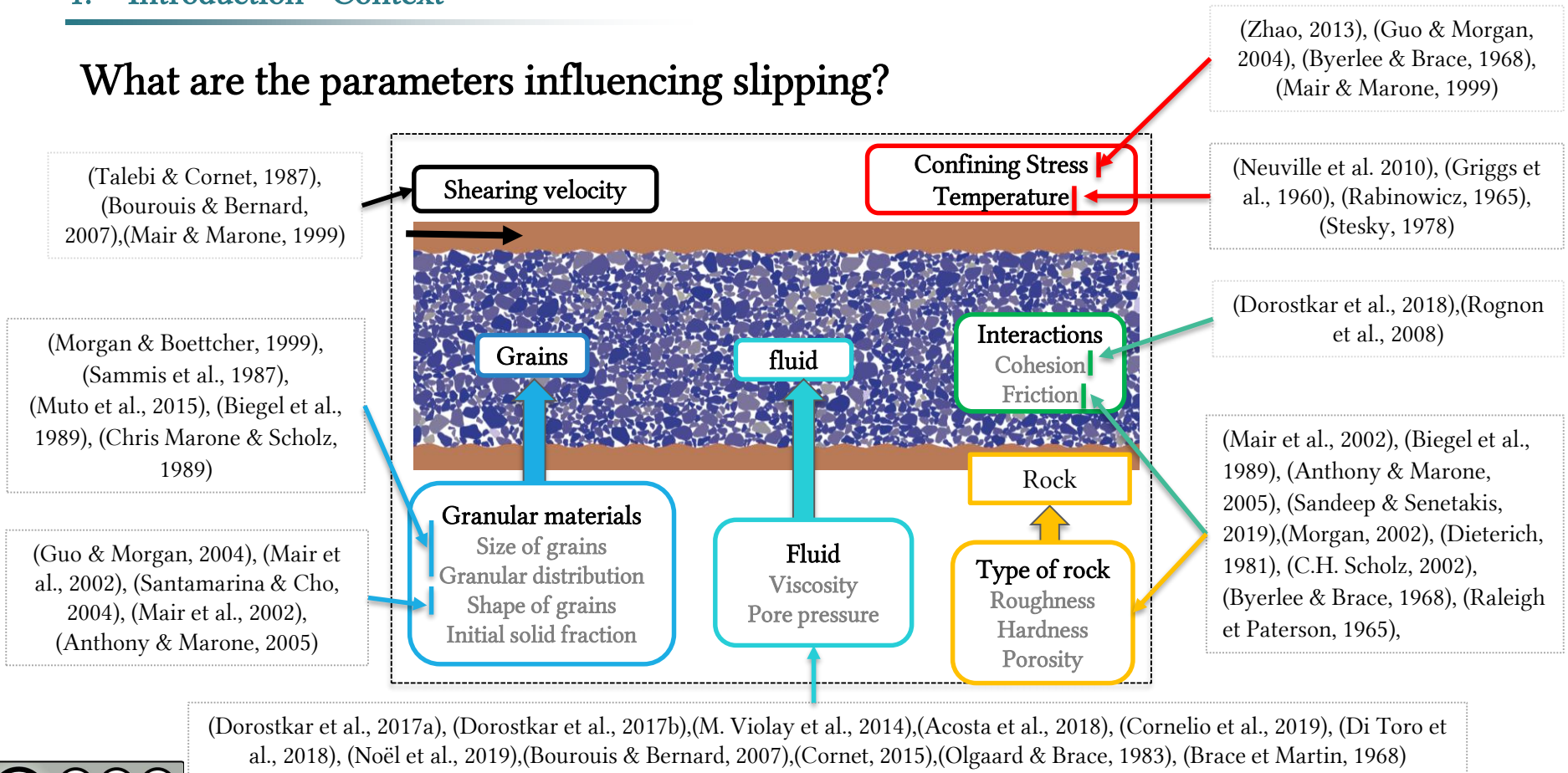
1. Introduction - Context

What is induced seismicity ?

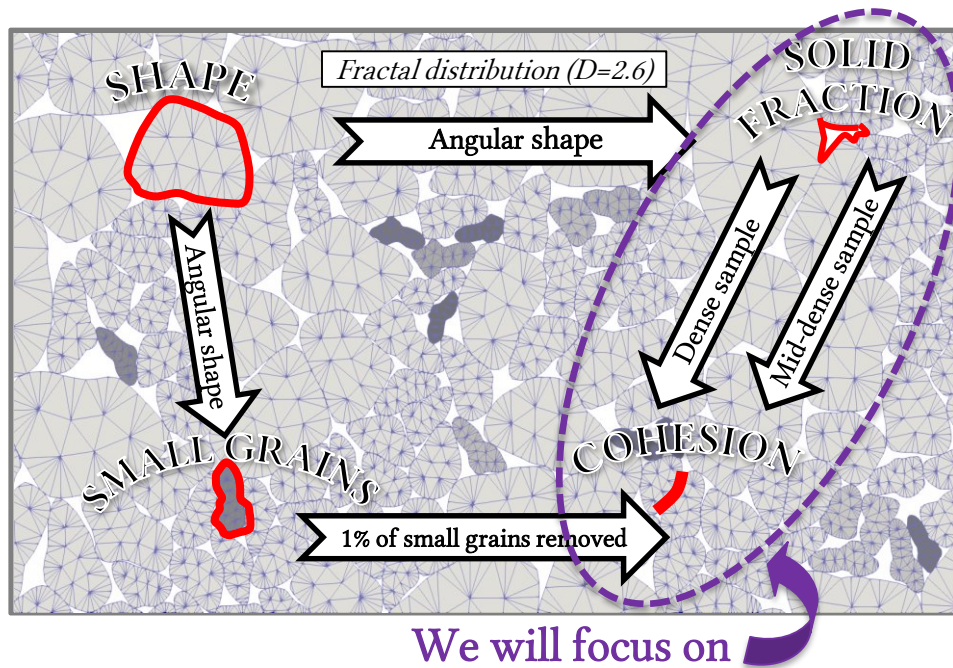


1. Introduction - Context

What are the parameters influencing slipping?



Overview of the investigated parameters



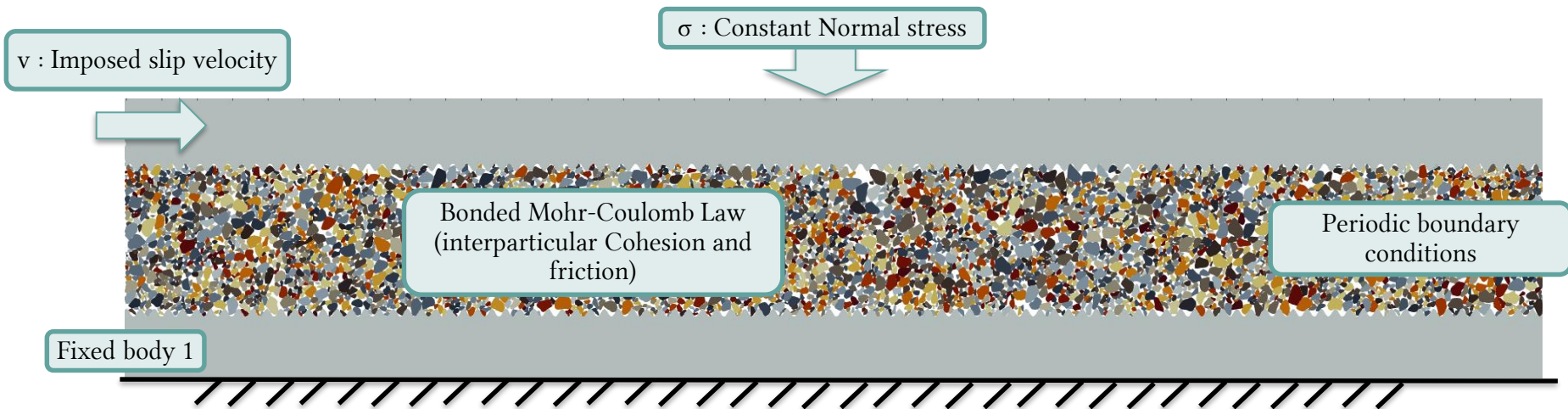
What is the influence of inter-particle friction within the gouge ?

- What is the role of cohesion? What does cohesion represent in reality and how can we simulate its effect?
- What is the influence of cohesion on the mechanical behavior of a granular fault gouge and on the energy budget of the system?
- Is the energy budget well defined and exhaustive? How can we enrich energy budget definition?

1. Introduction - Context

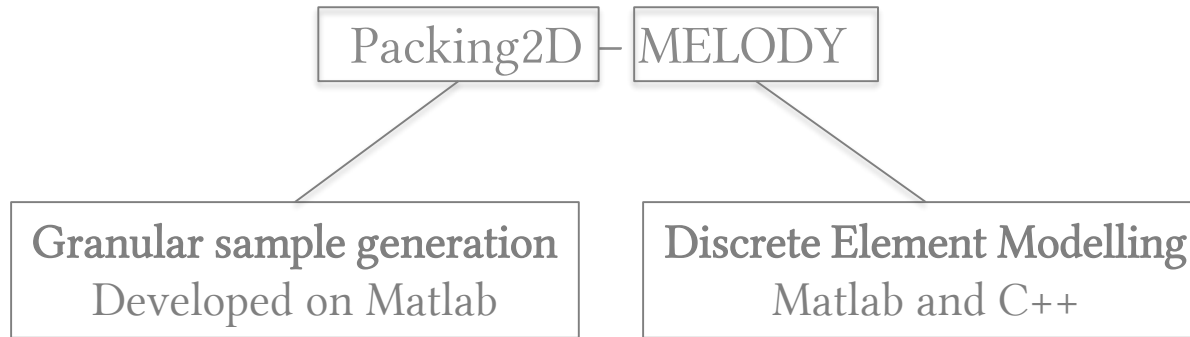
How to model a granular fault gouge ?

Discrete Element modelling – 2D – Granular and faceted shapes



➡ What is the influence of cohesion within the gouge?

2 – Sample generation and numerical modelling



(Mollon & Zhao, 2013)

Documented and free access

(Mollon, 2016), (Mollon, 2018a), (Mollon, 2018b)

2. Numerical modelling and sample generation

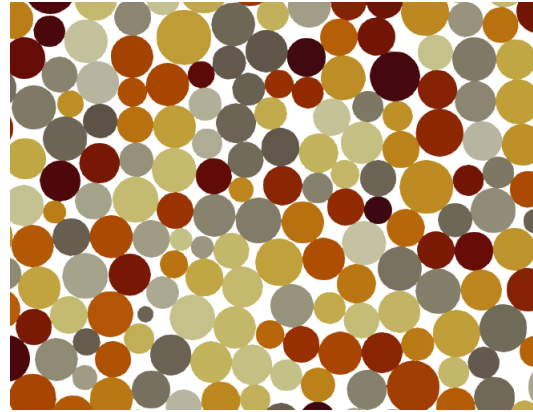
2.1- Packing2D

Generation of a realistic packing of grains with complex and angular shapes.

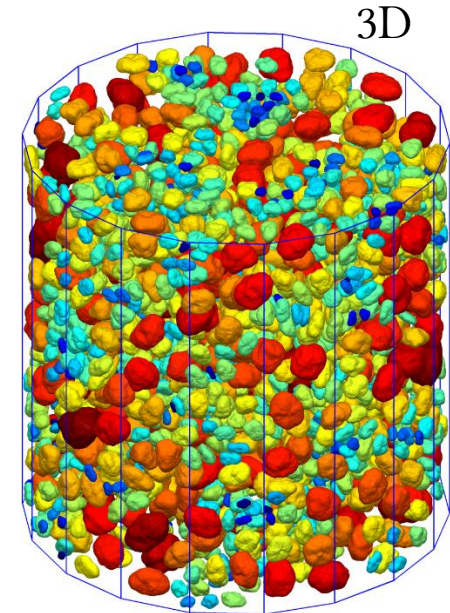
- Fourier-Voronoi method (2D) or (3D)
- Complex particle shapes
- Anisotropic orientation possible



2D



What is Packing 2D?



Mollon and Zhao, 2014

2. Numerical modelling and sample generation

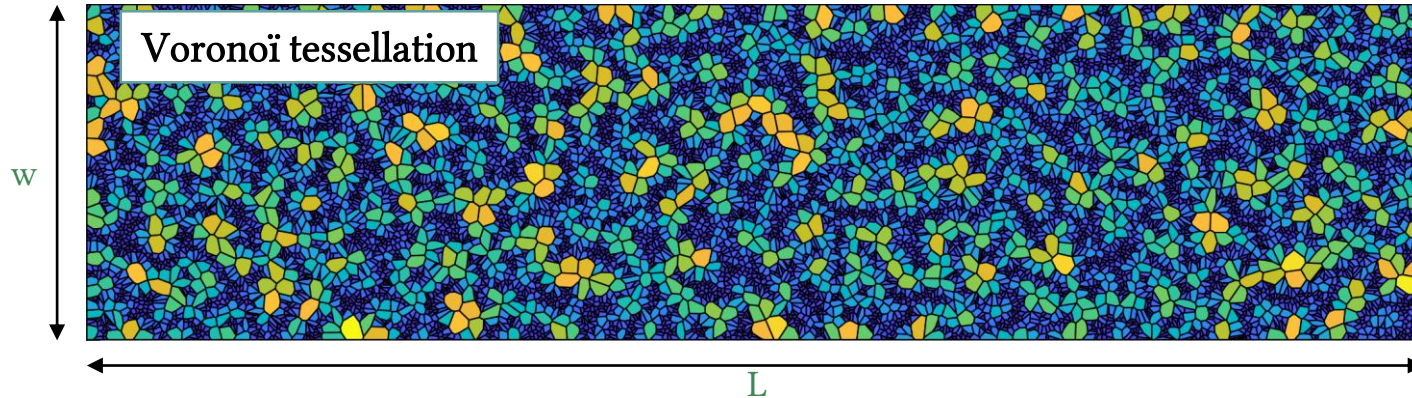
2.1- Packing2D

Step 1 : Generation of a Voronoï Tessellation

- Creation of the domain ($w \times L$)
- Division of the domain into N small cells
- Evaluation of the target size distribution

How to create a packing of grains?

Bounded Voronoï tessellation
+
Inverse Monte-Carlo Method



2. Numerical modelling and sample generation

2.1- Packing2D

How to create a packing of grains?

Step 2 : Spectrum of morphological descriptors, Fourier descriptors

Discrete Fourier spectrum of the signal $\{A_n, B_n\}$, fourier series:

$$r_i(\theta_i) = r_o + \sum_{n=1}^N [A_n \cos(n\theta) + B_n \sin(n\theta)] \text{ (with } r_o \text{ average radius)}$$

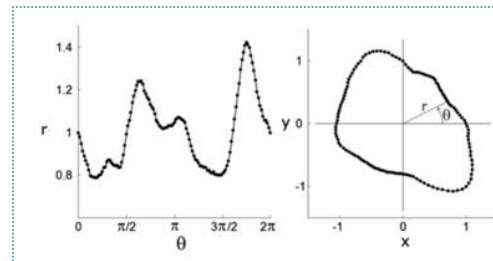
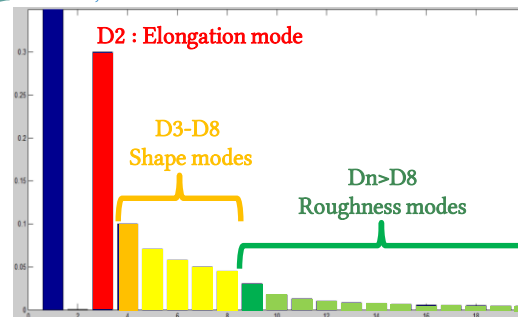
Normalized amplitude for each harmonics n:

$$D_n = \frac{\sqrt{A_n^2 + B_n^2}}{r_o} \rightarrow \text{“Fourier descriptor”}$$

N harmonics = N points to discretized the contour of grains.

Inverse Fourier transform \rightarrow *grain shape*

$D_0=1$, normalisation

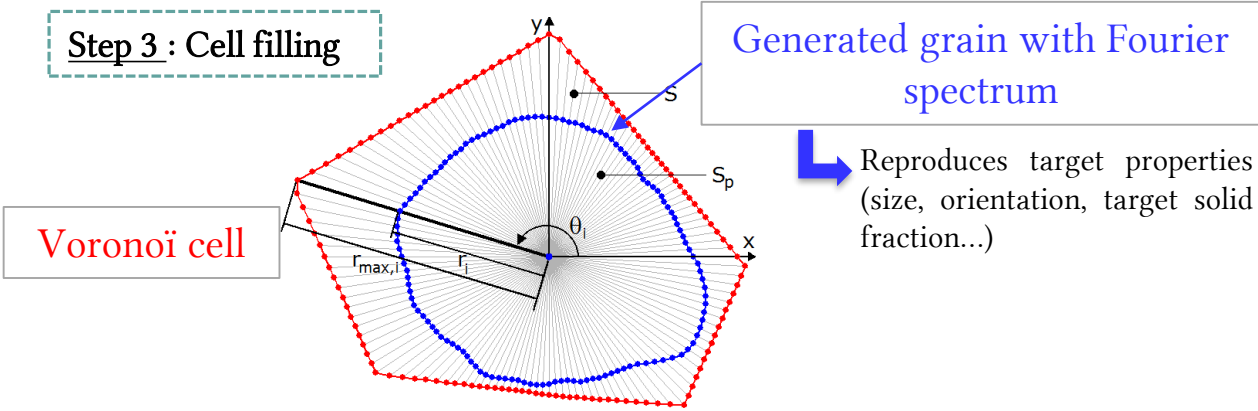


2. Numerical modelling and sample generation

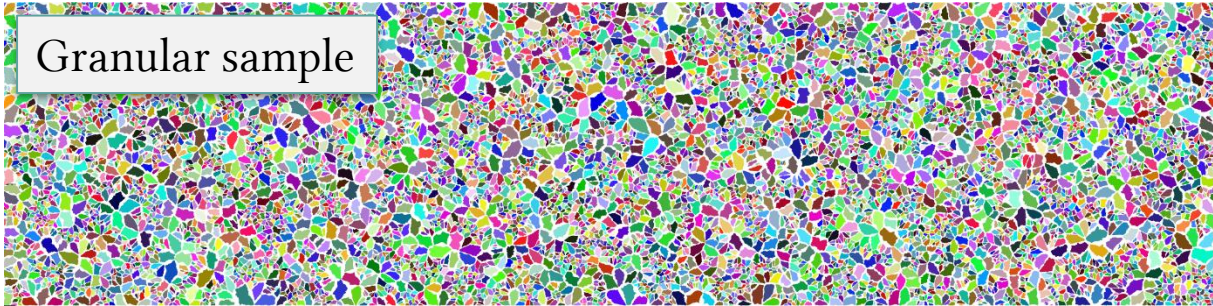
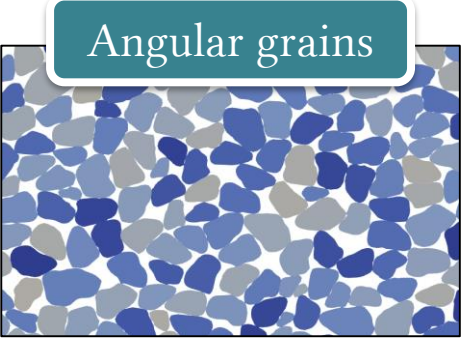
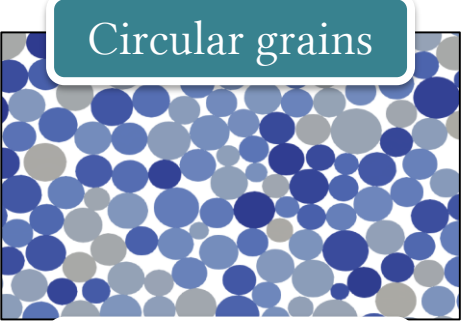
How to create a packing of grains?

2.1- Packing2D

Step 3 : Cell filling



Voronoi cell



2. Numerical modelling and sample generation

2.2- MELODY 2D

What are the advantages of DEM?

Discretized Element Method = DEM

DEM



- To compute motions of a large number of particles
- Every particle is considered as a body with dynamic equations
- Interactions with other bodies

MELODY = Multibody ELEMENT-free Open code for DYNAMIC simulation (Mollon, 2018)

Represent in the same digital frame the first and 3rd bodies with their deformation and dynamics

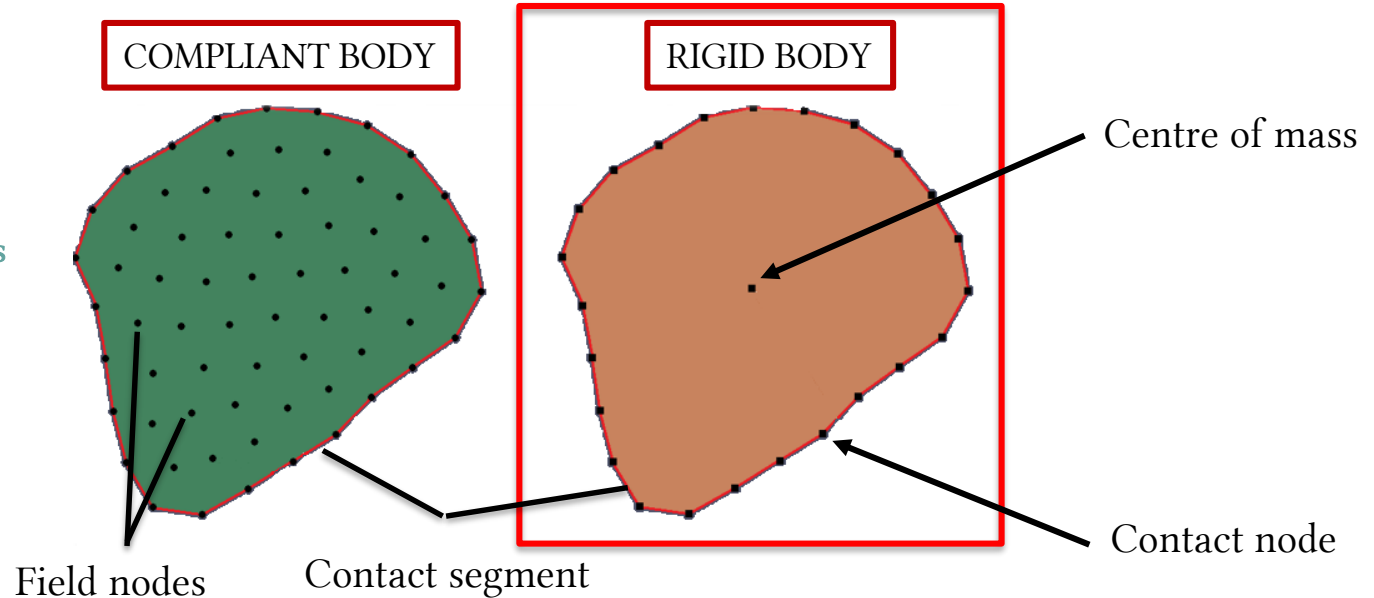
- to keep the discontinuity of the 3rd body => **Multi-body**
- to take into account the inertial and damping effect => **dynamic**

2. Numerical modelling and sample generation

2.2- MELODY 2D

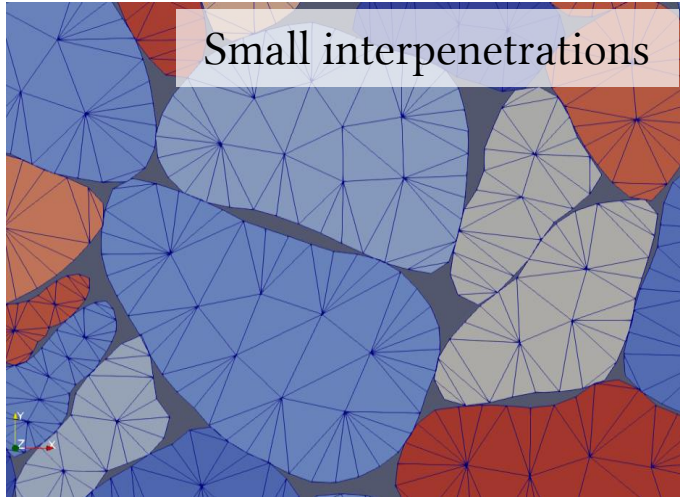
What is MELODY, what differences?

Mesh-free shape functions
(for compliant bodies)



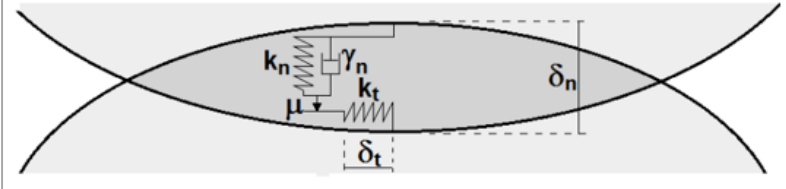
2. Numerical modelling and sample generation

2.2- MELODY 2D



What is MELODY, what differences?

$$F_n = \begin{cases} 0 & \text{si } \delta_n > 0 \\ -k_n \cdot \delta_n - \gamma_n \cdot \frac{d\delta_n}{dt} & \text{si } \delta_n < 0 \end{cases}$$
$$F_t = \begin{cases} -k_t \cdot \delta_t & \text{si } |-k_t \cdot \delta_t| \leq \mu \cdot F_n \\ \text{sign}(-k_t \cdot \delta_t) \cdot \mu \cdot F_n & \text{si } |-k_t \cdot \delta_t| > \mu \cdot F_n \end{cases}$$



Rigid grains → High numerical stiffness

Optimized proximity and contact detection → 3 steps of contact detection

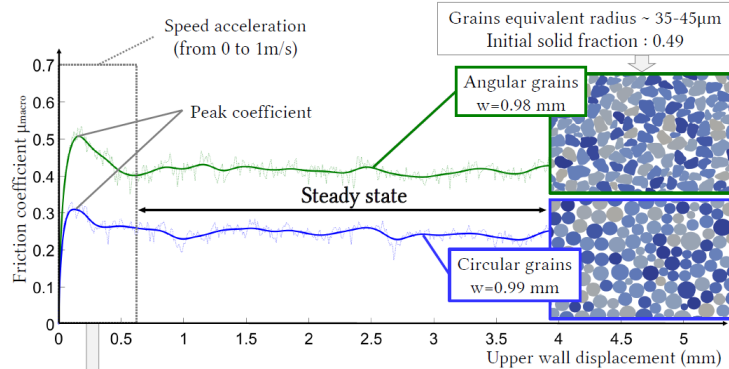
2. Numerical modelling and sample generation

2.3- Gouge model assumptions

What assumptions?

Shape and geometry of the model

- **Angular shapes of particles:** higher friction coefficient and different global behaviour from circular particles (Mair et al., 2002), (Guo et al., 2004). Validation with DEM



- **Size of the model:** 2D, 2mm x 20mm
- **Wavelength of the wall roughness:** sinusoidal

Rigid particles and bodies

Micromechanical point of view, deformation represented by numerical stiffness and interpenetration between particles. Less calculation cost. No fragmentation.

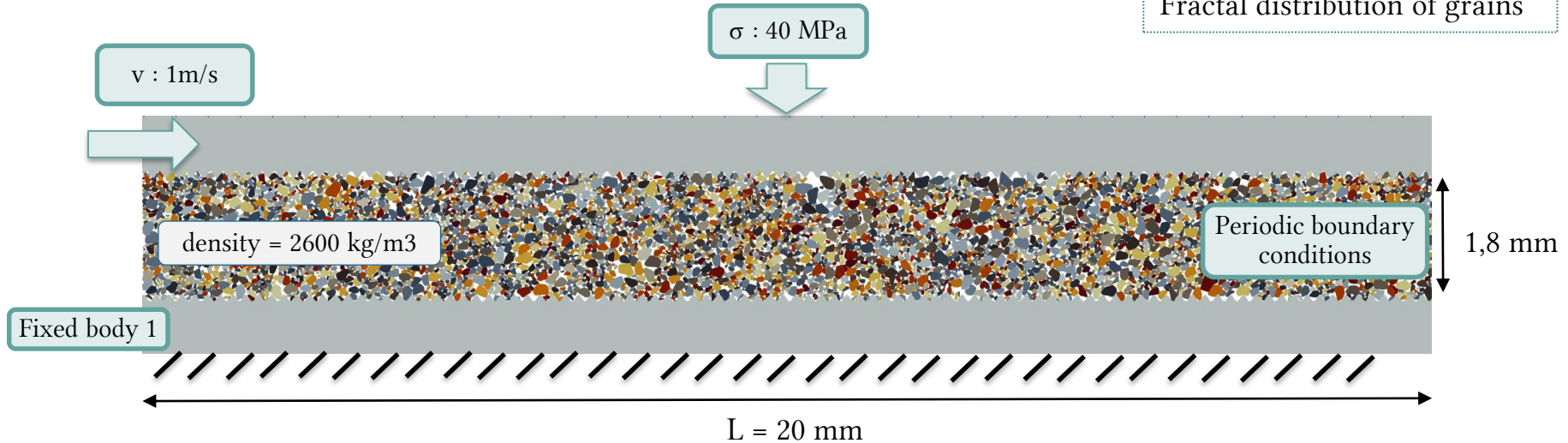
Contact detection and interaction

- **Dry contacts:** understand mechanism without water and test the effect of cohesion.
 - **Bonded Mohr-Coulomb contact law:**
 - Unbroken bond: constant value of cohesion
 - Broken bond: only inter-particle friction ($\mu_{micro}=0.5$)
- At the beginning of the experiment, all the particles in contact receive a percentage of cohesion. Once broken, a cohesive contact cannot be cohesive anymore.

2. Numerical modelling and sample generation

2.4- Procedures and boundary conditions

Number of particles: 4959
Size of particles: 27 – 260 μm
Fractal distribution of grains



Law: « Bonded Mohr-Coulomb »
Cohesion and friction between the
different bodies in contact.

Numerical stiffness and damping

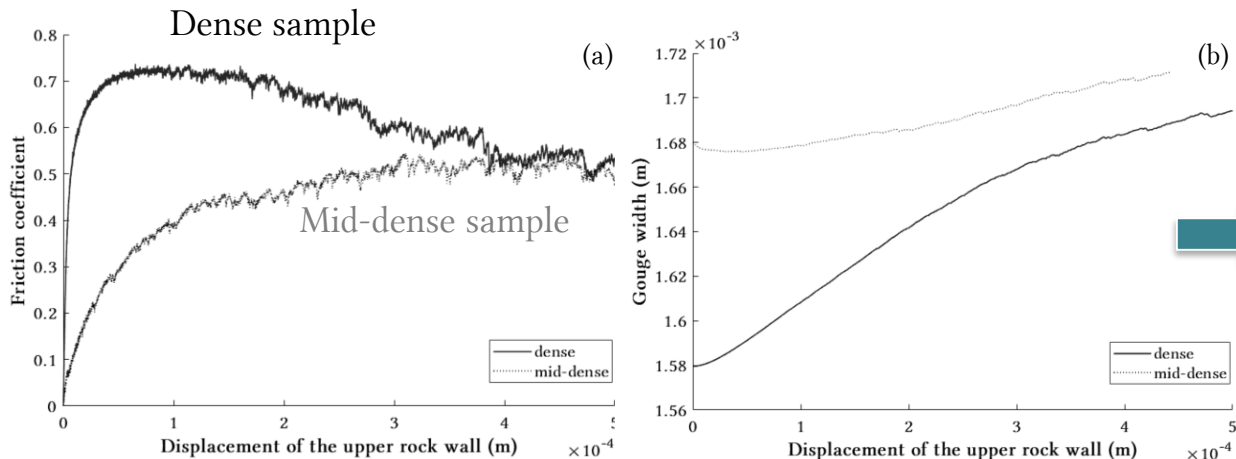
Inter-particle friction and cohesion

3 – Results on granular gouge behaviour

3. Results on granular gouge behavior

3.1- Initial solid fraction without cohesion

Solid fraction vs mechanical behaviour



Two kinds of initial samples:
dense and mid dense samples
→ Two mechanical behaviours

Graph 1: Shearing experiment of a granular fault gouge (a) Friction coefficient in function of the slip of the upper rock wall (m) - (b) Gouge width (m) in function of the slip of the upper rock wall (m) - for dense and mid-dense sample

Macroscopic friction

$$\mu(t) = \frac{F_T(t)}{F_N(t)}$$

Solid fraction

$$SF = \frac{S_{grains}}{S_{gouge}}$$

With $S_{gouge} = S_{grains} + S_{void}$

Dense sample, SF=0,89
Mid-dense sample, SF=0,84

3. Results on granular gouge behavior

3.2- Role of inter-particle cohesion

What is the effect of cohesion on granular gouge behavior? Cohesion is a difficult parameter to observe and to quantify and even more to follow during experiments. People have already tried to describe cohesion, from lab experiments or simulations (Rognon et al., 2008) with numerical cohesion or (Dorostkar et al., 2018) to represent capillary bridges. Here we try to bring some new knowledge on this parameter.

We decided to consider cohesion as a cementation we can find within a gouge, representing mineral matrix between particles.

Main differences with previous studies

- To use angular and faceted shapes instead of circular shapes
- To follow cohesion during the experiment
- To extract the energy budget from the breakage of cohesion bonds

Two kinds of initial samples:

- Dense SF=0,89
- Mid-dense SF=0,84

Cohesion quantification:

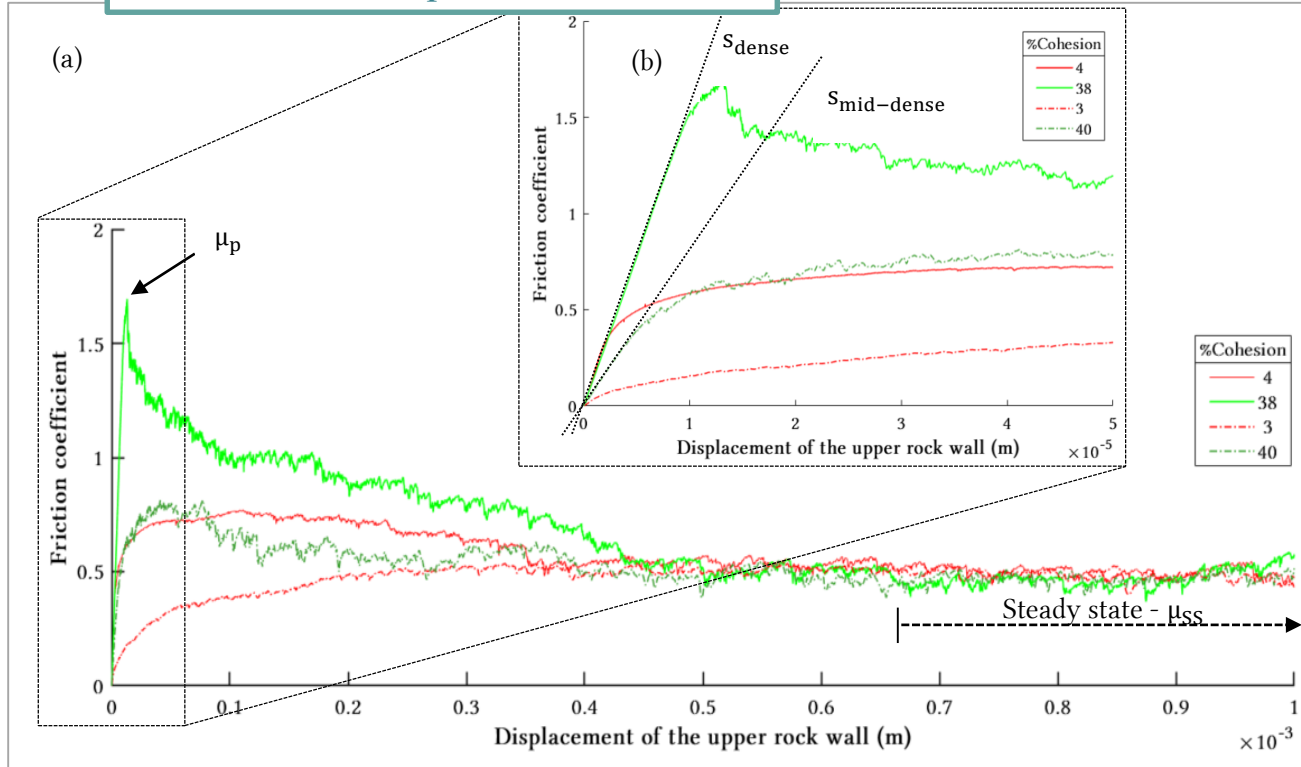
(Friedman et al., 1972) defined maximum cohesion and apparent surface energy of rocks, the energy needed to propagate a stable tensile fracture inside the rock. The higher apparent surface energy is found for the Chilhowee quartzite with a value of $U = 62 J.m^2$. We consider this energy as the maximum energy, where cohesion recovers 100% of grains perimeter.

We express cohesion as a percentage of cohesion $X\%$ inside the model, compared to the maximum cohesion found in our model for an energy U .

3. Results on granular gouge behavior

Friction coefficient

3.2- Role of inter-particle cohesion



Two kinds of initial samples:

- Dense SF=0,89
- Mid-dense SF=0,84

For a denser sample ?

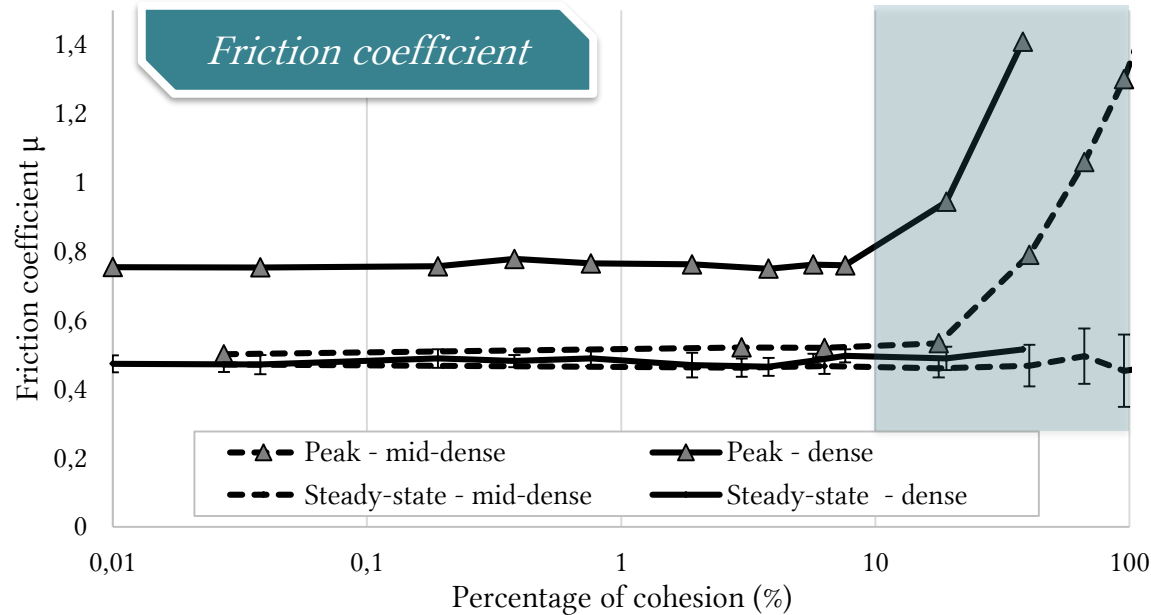
- Higher friction peak μ_p for the same % of cohesion
- Different peak shape
- Different initial slope
- Different critical slip distance
- Same average friction coefficient in the steady-state zone (0,5)
- Higher dilatancy rate

Friction curve comparison between dense and mid-dense sample in function of the upper wall displacement -

(b) Zoom in on the friction peak

3. Results on granular gouge behavior

3.2- Role of inter-particle cohesion



Shearing of a granular gouge - Friction coefficient (peak and average steady state) in function of the percentage of cohesion in the model – dense and mid-dense sample.

Non-cohesive behaviours [0–10% cohesion]:

- almost all cohesive bonds break at the beginning and give way to a Mohr-Coulomb contact law with inter-particle friction only.
- Behaviour very close to a non-cohesive gouge respectively for dense and mid-dense sample.

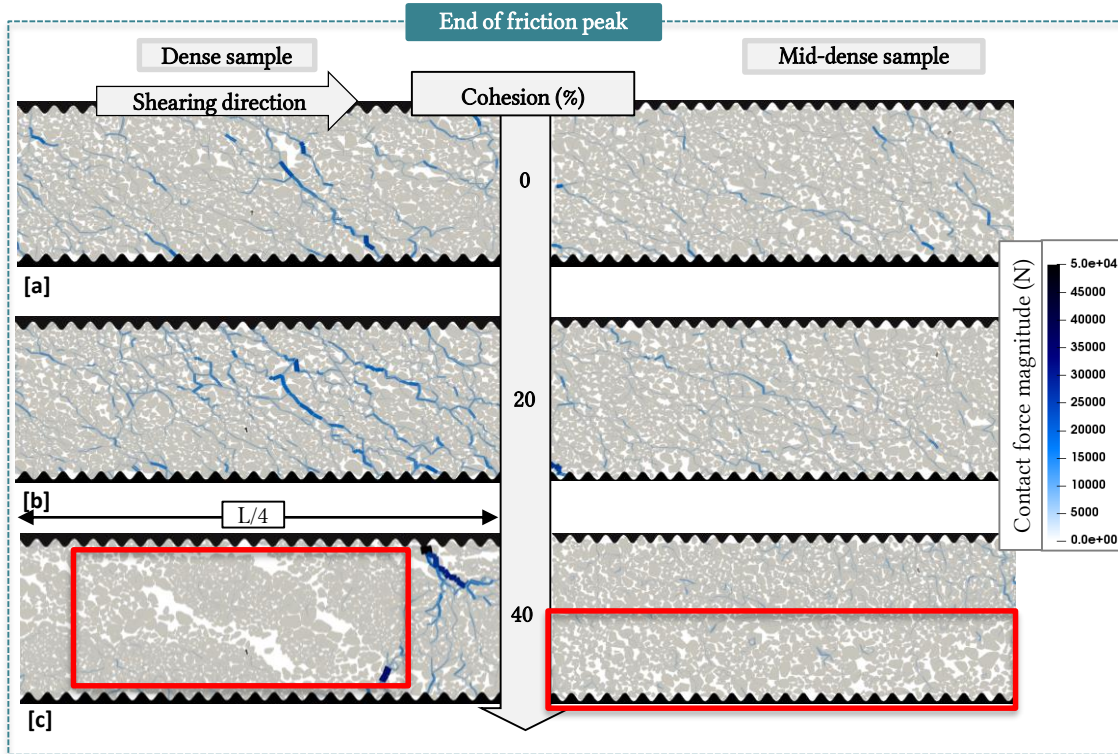
Cohesive behaviours [>10% cohesion]:

- Some cohesive bonds remain intact during the beginning of shearing.
- Cohesion modifies the initial state of compaction and the energy that the system must provide to break the tangled and cohesive grains.
- High cohesion contacts occur between agglomerates of cohesive grains, changing the whole geometry and PSD of the gouge.

3. Results on granular gouge behavior

3.2- Role of inter-particle cohesion

Force chains and solid fraction



Different fracturation behaviours inside the granular gouge. For 40% of cohesion:

- Dense: shear bands in the direction of force chains, increase of porosity inside the sample. Clusters of cohesive grains.
- Mid-dense: Shearing localization at the bottom of the sample. Big cohesive zone in the upper part of the gouge.

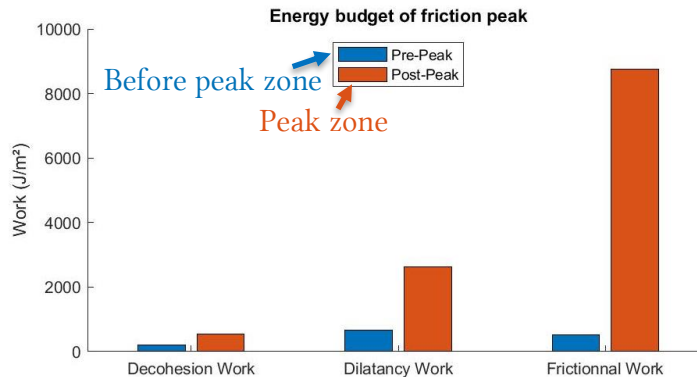
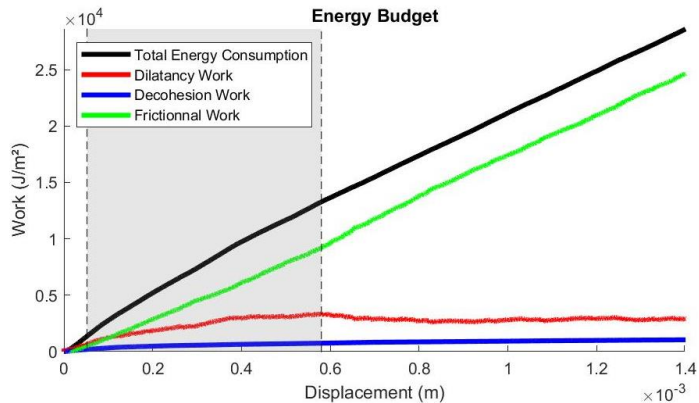
→ Initial solid fraction of the sample changes packing of particles, and thus the application of cohesion. Shear bands do not follow the same patterns.

3. Results on granular gouge behavior

Energy Budget – new definition

3.2- Role of inter-particle cohesion

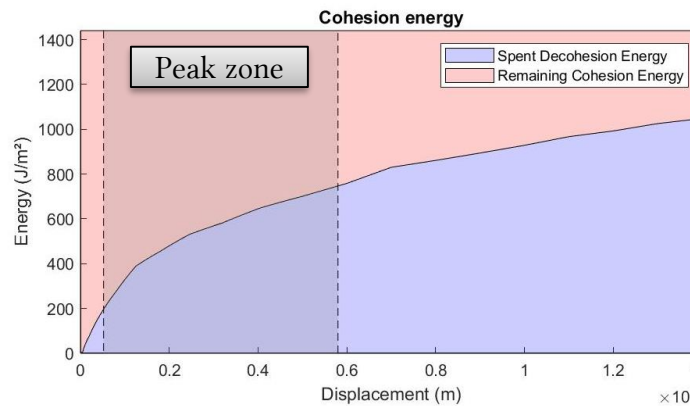
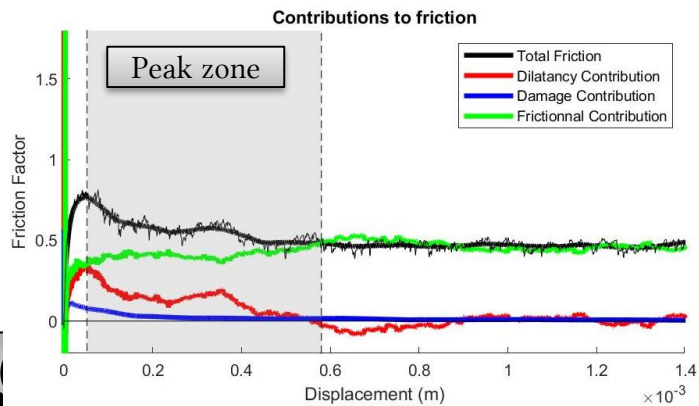
Example for a mid-dense sample – 40% cohesion



Dilatancy contribution = from the dilation of the gouge.

Damage contribution = from the energy used to break cohesive bonds.

Frictional contribution = from the inner friction between particles.



3. Results on granular gouge behavior

Energy Budget – new definition

3.2- Role of inter-particle cohesion

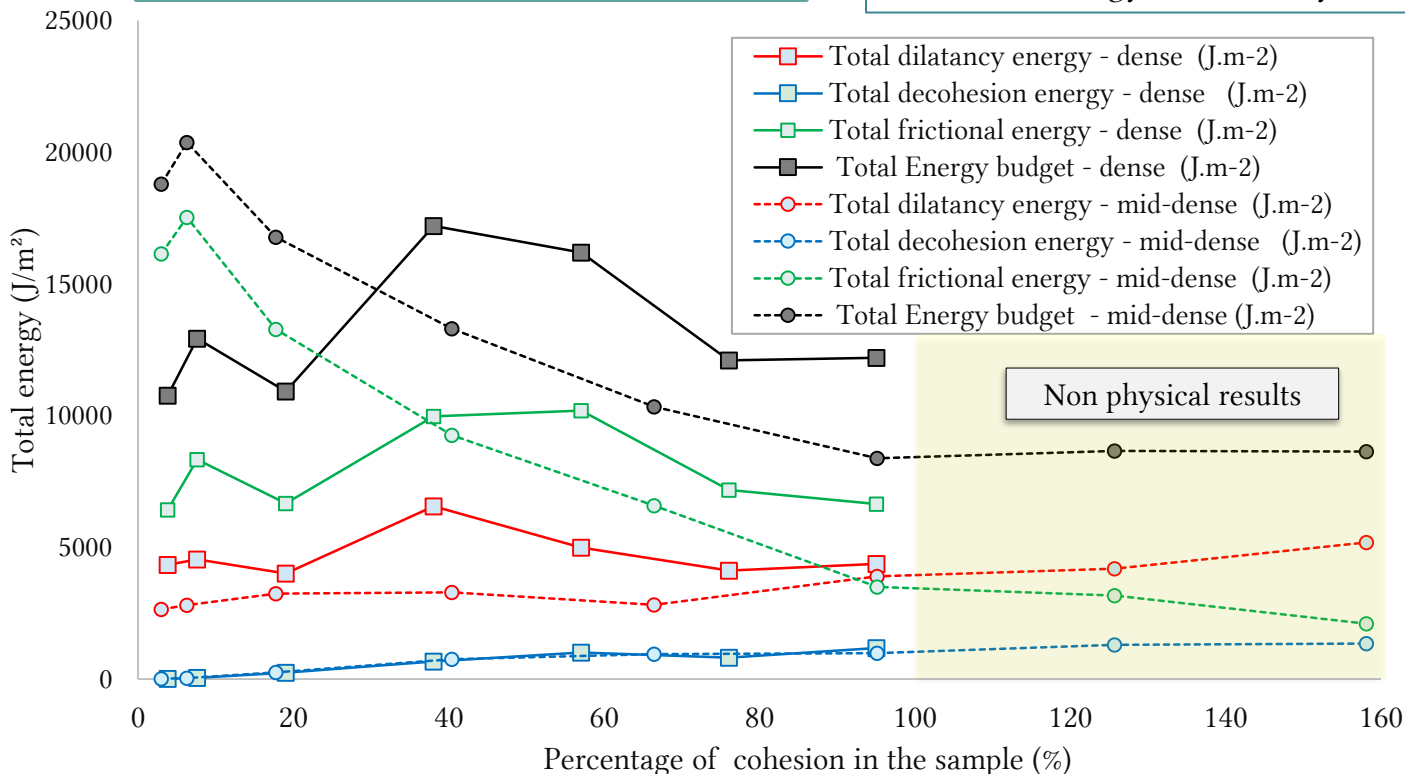
Frictional Energy \geq Dilatancy Energy \geq Decohesion Energy



Dense sample: more energy needed after 40% cohesion. But cohesion doesn't seem to have a big influence on energy budget.

Mid-dense sample: energy needed by the system decreases from 0 to 100% cohesion, getting closer to the energy needed by a denser sample.

What part in Fracture Energy?
How can we relate this new Energy budget and Fracture Energy?



Non physical results



3. Results on granular gouge behavior

3.2- Role of inter-particle cohesion

Conclusion

- **For small or non-cohesive gouge** [0 – 10% cohesion]

Mechanical behaviour of the granular gouge is similar between 0 and 10% cohesion, we can conclude that the effect of cohesion is negligible below 10% for the given experimental conditions. Cohesive bonds break very quickly when the upper wall is set in motion, reducing the tests to standard tests without cohesion. Normal stress and imposed velocity on the upper rock wall generate larger efforts in the gouge than the inter-particle cohesion.

- **For cohesive gouge** [>10% cohesion]

The observed peak of friction is much more important because, before expanding, the system must be able to break cohesive bonds. Once the sample is "fractured", the gouge will expand and tend towards an average friction value on steady-state part, similar to the one observed for cases without cohesion. Cohesive bonds are however always present after the friction peak, maintaining clusters of cohesive grains inside the gouge. Solid fraction decreases in the case of a very cohesive gouge, and fracture opening can lead to a more permeable gouge.

- Friction differences between dense and mid-dense sample increase with a higher percentage of cohesion. A denser sample presents higher friction coefficient, but shear band localisation tend to break the gouge in a different way. (Marone et al 1990) remind us that granular fault gouges involving dilation during shear produce velocity-strengthening frictional behaviour. (Beeler et al, 1996) also reported that friction velocity can be related to dilatancy rate. Strengthening behaviour is observed for higher dilatancy and Riedel shear bands R1. However, a higher cohesion seems to bring closer energy budget of dense and mid-dense samples.

- Cohesion also increases this strengthening behaviour, cementing the initial sample. Knowing the cohesion within the gouge can let us have a better idea of the strengthening or weakening behaviour of a granular fault gouge. Studying more in details friction peak could give us information about dynamic of the gouge, and link microstructures to seismic and aseismic behaviours.

4- Conclusion and perspectives

- 2D Discrete Element modelling with angular and faceted shapes
 - Role of cohesion in the mechanical behaviour of the granular gouge
 - A certain percentage of cohesion is needed to affect the gouge (>10%)
 - The increase of cohesion changes fracturation mechanisms inside the granular gouge and leads to brittle behaviours.
 - During the peak zone, the energy budget of the gouge get closer for dense and mid-dense samples after 40% of cohesion.
 - On-going work on a new definition of energy budget and fracture energy linked to micro-mechanical behaviour
-
- Next:
 - Represent mineral matrix between particles, and study the shear band localisation
 - Rock walls need to be deformable to represent stiffness of the loading apparatus
 - New model with elastic medium and pressure gradient to simulate the increase of pore pressure and observation of slip triggering

Bibliography

1. Morgan JK, Boettcher MS. Numerical simulations of granular shear zones using the distinct element method: 1. Shear zone kinematics and the micromechanics of localization. *J Geophys Res Solid Earth* [Internet]. 1999;104(B2):2703–19. Available from: <http://doi.wiley.com/10.1029/1998JB900056>
2. Sammis C, King G, Biegel R. The kinematics of gouge deformation. *Pure Appl Geophys PAGEOPH*. 1987;125(5):777–812.
3. Muto J, Nakatani T, Nishikawa O, Nagahama H. Fractal particle size distribution of pulverized fault rocks as a function of distance from the fault core. *Geophys Res Lett*. 2015;42(10):3811–9.
4. Biegel RL, Sammis CG, Dieterich JH. The frictional properties of a simulated gouge having a fractal particle distribution. *J Struct Geol*. 1989;11(7):827–46.
5. Marone C, Scholz CH. Particle-size distribution and microstructures within simulated fault gouge. *J Struct Geol*. 1989;11(7):799–814.
6. Guo Y, Morgan JK. Influence of normal stress and grain shape on granular friction: Results of discrete element simulations. *J Geophys Res Solid Earth*. 2004;109(12):1–16.
7. Mair K, Frye KM, Marone C. Influence of grain characteristics on the friction of granular shear zones. *J Geophys Res Solid Earth* [Internet]. 2002;107(B10):ECV 4-1-ECV 4-9. Available from: <http://doi.wiley.com/10.1029/2001JB000516>
8. Santamarina JC, Cho GC. Soil behaviour: The role of particle shape. *Proc a Three Day Conf Adv Geotech Eng*. 2004;604–17.
9. Anthony JL, Marone C. Influence of particle characteristics on granular friction. *J Geophys Res Solid Earth*. 2005;110(8):1–14.
10. Byerlee JD, Brace WF. Stick slip, stable sliding, and earthquakes—Effect of rock type, pressure, strain rate, and stiffness. *J Geophys Res* [Internet]. 1968;73(18):6031–7. Available from: <http://doi.wiley.com/10.1029/JB073i018p06031>
11. Zhao Z. Gouge particle evolution in a rock fracture undergoing shear: A microscopic DEM study. *Rock Mech Rock Eng*. 2013;46(6):1461–79.
12. Mair K, Marone C. Friction of simulated fault gouge for a wide range of velocities and normal stresses. *J Geophys Res Solid Earth* [Internet]. 1999 Dec 10 [cited 2019 Jan 3];104(B12):28899–914. Available from: <http://doi.wiley.com/10.1029/1999JB900279>
13. Talebi S, Cornet FH. Analysis of the microseismicity induced by a fluid injection in a granitic rock mass. *Geophys Res Lett*. 1987;14(3):227–30.
14. Bourouis S, Bernard P. Evidence for coupled seismic and aseismic fault slip during water injection in the geothermal site of Soultz (France), and implications for seismogenic transients. *Geophys J Int*. 2007;169(2):723–32.
15. Sandeep CS, Senetakis K. An experimental investigation of the microslip displacement of geological materials. *Comput Geotech* [Internet]. 2019;107(June 2018):55–67. Available from: <https://linkinghub.elsevier.com/retrieve/pii/S0266352X18302945>

Bibliography

16. Morgan JK. Numerical simulations of granular shear zones using the distinct element method: 2. Effects of particle size distribution and interparticle friction on mechanical behavior. *J Geophys Res Solid Earth*. 2002;104(B2):2721–32.
17. Neuville A, Toussaint R, Schmittbuhl J. Fracture roughness and thermal exchange: A case study at Soultz-sous-Forêts. *Comptes Rendus - Geosci*. 2010;342(7–8):616–25.
18. Dorostkar O, Guyer RA, Johnson PA, Marone C, Carmeliet J. On the micromechanics of slip events in sheared, fluid-saturated fault gouge. *Geophys Res Lett*. 2017;44(12):6101–8.
19. Dorostkar O, Guyer RA, Johnson PA, Marone C, Carmeliet J. On the role of fluids in stick-slip dynamics of saturated granular fault gouge using a coupled computational fluid dynamics–discrete element approach. *J Geophys Res Solid Earth*. 2017;122(5):3689–700.
20. Violay M, Nielsen S, Gibert B, Spagnuolo E, Cavallo A, Azais P, et al. Effect of water on the frictional behavior of cohesive rocks during earthquakes. *Geology*. 2014;42(1):27–30.
21. Violay M. Coupled Hydro-mechanical processes in fault zones , implications for deep geothermal reservoirs.
22. Acosta M, Passelègue FX, Schubnel A, Violay M. Dynamic weakening during earthquakes controlled by fluid thermodynamics. *Nat Commun* [Internet]. 2018;9(1). Available from: <http://dx.doi.org/10.1038/s41467-018-05603-9>
23. Cornelio C, Spagnuolo E, Di Toro G, Nielsen S, Violay M. Mechanical behaviour of fluid-lubricated faults. *Nat Commun*. 2019;10(1):1–7.
24. Di Toro G, Spagnuolo E, Violay M, Passelègue F, Cornelio C. Fluid viscosity controls earthquakes nucleation. In: *Rendiconti Lincei*. 2018.
25. Noël C, Pimienta L, Violay M. Time-Dependent Deformations of Sandstone During Pore Fluid Pressure Oscillations: Implications for Natural and Induced Seismicity. *J Geophys Res Solid Earth*. 2019;124(1):801–21.
26. Cornet FH. Earthquakes induced by fluid injections. *Science* (80-). 2015;348(6240):1204–5.
27. Olgaard DL, Brace WF. The microstructure of gouge from a mining-induced seismic shear zone. *Int J Rock Mech Min Sci*. 1983;20(1):11–9.
28. Frye KM, Marone C. The effect of particle dimensionality on Granular friction in laboratory shear zones. *Geophys Res Lett*. 2003;29(19):22-1-22–4.
29. G. Mollon, J. Zhao, Fourier-Voronoi-based generation of realistic samples for discrete modelling of granular materials, *Granul. Matter*. (2012) 621–638. doi:10.1007/s10035-012-0356-x
30. G. Mollon, A unified numerical framework for rigid and compliant granular materials, *Comput. Part. Mech.* (2018) 1–11. doi:10.1007/s40571-018-0187-6.
31. C.H. Scholz, *The Mechanics of Earthquakes and Faulting*, second edition, Cambridge, 2002